DIVISION OF
FLUID, THERMAL AND AEROSPACE SCIENCES

SCHOOL OF ENGINEERING

CASE WESTERN RESERVE UNIVERSITY

CONDENSATION HEAT TRANSFER OF LOW PRESSURE METAL VAPORS

by

Yun-Seng Huang, Frederic A. Lyman, and Wilbert J. Lic

UNIVERSITY CIRCLE • CLEVELAND, OHIO 44106

FTAS/TR-70-54

CONDENSATION HEAT TRANSFER OF LOW PRESSURE METAL VAPORS

by

Yun-Seng Huang, Frederic A. Lyman, and Wilbert J. Lick

January 1971

ABSTRACT

This thesis is concerned with the film condensation of low pressure metal vapors on isothermal vertical flat plates or tubes. The liquid film has been treated as a thin layer in which the acceleration and pressure forces are negligible and across which the temperature distribution is linear. The average behavior of the vapor has been found from the linearized one-dimensional vapor flow equations. A consistent distribution function has been determined for the vapor particles at the liquid-vapor interface.

The result of this analysis is a set of algebraic equations from which one can predict the condensation rate of low pressure metal vapors. There is good agreement between the most recent and reliable experimental data and the present theoretical calculations if, in the present calculations, the presence of a small amount of a noncondensible gas is included.

ACKNOWLEDGMENTS

The author especially thanks his co-advisors, Professor Frederic A. Lyman, who introduced him to the condensing metals problem and gave his every assistance to seeing the program underway, and Professor Wilbert J. Lick, who entered the program in Dr. Lyman's absence and has also given freely of his time and knowledge in all phases of the study.

The author is also gratefully indebted to Professor B. Samuel Tanenbaum for his assistance and discussion of the section on the distribution function.

The author wishes to acknowledge the support provided for this study by Lewis Research Center under NASA Grant NGR-36-003-064.

TABLE OF CONTENTS

LIST OF FIGURES

LIST OF SYMBOLS

A	integration constant appearing in Eq. (2.3.18)
A_g	total amount of noncondensible gases per unit area of condensing surface
a_s	thermal agitating speed defined by Eq. (2.4.7)
B	integration constant appearing in Eq. (2.3.19)
C	molecular speed
c_1	integration constant defined by Eq. (2.3.9)
c_2	integration constant defined by Eq. (2.3.11)
c_p	specific heat of vapor or mixture
c_{pl}	specific heat of condensate
D_{12}	diffusion coefficient of a mixture of two components
f	distribution function of particles at the liquid-vapor interface
f_1	component of distribution function defined by Eq. (2.4.3)
f_2	component of distribution function defined by Eq. (2.4.4)
f_3	component of distribution function defined by Eq. (2.4.5)
G	local mass condensation rate per unit area
$\bar{G}$	average mass condensation rate per unit area
$\bar{G}_i$	average mass condensation rate per unit area at the interface
g	gravitational acceleration
$\bar{h}$	average heat transfer coefficient
$\bar{h}_{Nu}$	average Nusselt heat transfer coefficient
K	thermal conductivity of vapor or mixture

K_ℓ	thermal conductivity of condensate
K_n	Kundsen number
L	vertical length of condensing surface
M	molecular weight
M_∞	Mach number of mean vapor flow at infinity
m	mass of a molecule
n_s	saturation number density at temperature T_s
n_Δ	number density of particles of third kind
P	pressure of vapor or mixture
P_i	pressure of vapor at the interface
P_r	Prandtl number
P_v	pressure of vapor
P_{vi}	partial pressure of vapor at interface
P_s	saturation pressure at temperature T_s
Q	local heat flux per unit area
$\bar{Q}$	average heat flux per unit area
R	universal gas constant
R_M	gas constant of vapor or mixture
r	radial coordinate
r_c	radius of condensing tube
T	temperature of vapor or mixture
T_i	temperature of vapor at the interface
T_ℓ	temperature of condensate
T_v	temperature of vapor
T_s	temperature at the liquid-vapor interface

T_w	temperature on the wall
T_Δ	normal temperature of particles of third kind
T'	perturbation of vapor temperature
U	molecular velocity in x-direction
u_ℓ	velocity of condensate in x-direction
V	molecular velocity in y-direction
v	velocity of vapor or mixture in y-direction
v_d	mean drift velocity of particles of second kind
v_i	velocity of vapor at the interface
v_ℓ	velocity of condensate in y-direction
v'	perturbation of vapor velocity
W	concentration or mass fraction of air
$(\frac{W}{A})_{net}$	net rate of condensation
$(\frac{W}{A})_s$	absolute rate of evaporation
$(\frac{W}{A})_v$	absolute rate of condensation
x	direction parallel to liquid surface
y	direction normal to liquid surface
α	roots defined by Eq. (2.3.25)
β_{w_i}	dimensionless parameter defined by Eq. (3.33)
Γ	correction factor defined by Eq. (1.4)
γ	ratio of specific heats
δ_ℓ	local film thickness of liquid
$(\delta_\ell)_e$	effective film thickness
ε_{ij}	dimensionless parameter defined by Eq. (3.11)
λ	latent heat of condensation

k	Boltzmann's constant
μ	viscosity of vapor or mixture
μ_ℓ	viscosity of condensate
ν	kinematic viscosity of vapor or mixture
ν_ℓ	kinematic viscosity of condensate
ρ	density of vapor or mixture
ρ_i	density of vapor at the interface
ρ_ℓ	density of condensate
ρ_v	density of vapor
ρ_Δ	density of particles of the third kind
σ	diameter of molecule
σ_c	condensation coefficient
σ_e	evaporation coefficient
σ_H	coefficient defined by Eq. (2.4.19)
ϕ	dimensionless parameter defined by Eq. (1.5)
χ	normalized concentration distribution function

Subscripts

0	stagnation conditions
1	properties of vapor
2	properties of noncondensible gas
∞	conditions at infinity or at the intersection of outer and interfacial regions

Superscripts

0	zeroth order solution
1	first order solution
2	second order solution

I. INTRODUCTION

In many engineering applications, one encounters problems which require a thorough understanding of the transfer of mass, momentum, and energy between phases. One important example of this type of problem is the physical process of condensation; that is, the change of phase from vapor to liquid state. This phenomenon can occur whenever a saturated vapor comes in contact with a surface which is at a temperature lower than the saturation temperature of the vapor. If this is the case and condensation occurs, then the latent heat thereby liberated represents the major portion of the heat transferred.

Condensation on a cool surface is initially in the form of a large number of very small droplets which continue to grow by condensation and by coalescence with other neighboring droplets until the droplets start moving along the cool surface under the action of gravity and/or flowing vapor. New droplets will immediately continue to form in the trace behind the moving droplets. These moving droplets then join to form continuous streams and these streams in turn join with each other to eventually form a film over the entire cool surface. In the initial stage of condensation, we speak of dropwise condensation, while in the final stage, we speak of film condensation. The change-over from dropwise to film condensation will take place unless the cool surface is contaminated and/or a sizable amount of noncondensible gas is present in the system. The time needed for change-over depends on the wetting

properties of the vapor and condensing surface. Condensation of mercury vapor on a nickel surface may take as much as ten hours to change over to film condensation. In general, dropwise condensation can not be maintained for a long period of time, and therefore most condensing equipment is designed with the assumption that film condensation will exist. Thus, film condensation is of more practical importance.

Under conditions where the forced-convective velocities are negligible, the condensate formed on the cool surface will flow downward mainly under the influence of gravity. The flow of the condensate may be laminar or turbulent. The transition to turbulence will occur when the condensate layer grows sufficiently thick. However, the flow in the upstream portion of the condensate is still laminar. Fluid motions within the bulk of the vapor are caused by the removal of mass at the liquid-vapor interface, and by diffusion due to temperature and concentration differences. In some situations, the interfacial shear force may also become important.

Nusselt [1] developed a theory of steady-state, condensation heat transfer on an isothermal vertical surface. In his work, Nusselt made many restrictive assumptions, of which several have been removed in the past ten years. Nusselt's assumptions are:

1. There is no temperature drop in the bulk of the vapor; that is, the temperature on the surface of the liquid film is the temperature of the bulk vapor.

2. Subcooling of the condensate may be neglected.

3. The condensate flow is laminar.

4. The fluid properties are constant.

5. The inertia effects in the liquid film are negligible.

6. Vapor drag at the liquid-vapor interface may be neglected.

7. The temperature distribution in the film is linear.

With these assumptions, Nusselt derived the well-known formula,

$$\bar{h}_{Nu} = \frac{4}{3}\left[\frac{g\rho_\ell^3 K_\ell^3 \lambda}{4\mu_\ell L (T_s - T_w)}\right]^{\frac{1}{4}} \tag{1.1}$$

where

$\bar{h}_{Nu}$ = average heat transfer coefficient,

g = gravitational acceleration,

ρ_ℓ = density of the condensate,

K_ℓ = thermal conductivity of the condensate,

μ_ℓ = viscosity of the condensate,

λ = latent heat of condensation,

L = vertical length of condensing plate or tube,

T_s = surface temperature of liquid film,

T_w = temperature of the cold wall.

The first improvement in Nusselt's theory was made by Bromley [2]. He derived a correction to account for the effect of liquid subcooling. The improved analysis predicted a slight increase in heat transfer at high values of the parameter $C_{p\ell}\left(\frac{T_s - T_w}{\lambda}\right)$ where $C_{p\ell}$ is the specific heat of the condensate. In most applications,

this parameter is very small and has a value between 0 and 0.2.

Seban [3] extended Nusselt's theory to the case of higher Reynolds number by assuming a transition from laminar to turbulent flow at a Reynolds number of 1600 and a universal velocity distribution in the film. His results verified the qualitative expectation that, in turbulent flow, heat transfer coefficients were higher for large Prandtl number fluids (Pr = 0.5 or greater), but showed little change for low Prandtl number fluids.

The study of the effect of the nonlinear temperature distribution in the liquid film was first made by Rohsenow [4]. His analysis was similar to Bromley's and he improved Bromley's model by including the effect of cross flow within the film. He found that this refinement becomes important only for large values of the parameter $c_{p_\ell}\left(\frac{T_s - T_w}{\lambda}\right)$.

Further refinement of the Nusselt model, including momentum effects as well as energy convection, was made by Sparrow and Gregg [5] using a similarity transformation method. Solutions were obtained for values of the parameter $c_{p_\ell}\left(\frac{T_s - T_w}{\lambda}\right)$ between .003 and 100. It was found that the inclusion of the momentum terms had very little effect on the heat transfer for small values of the parameter $c_{p_\ell}\left(\frac{T_s - T_w}{\lambda}\right)$. Similar results were obtained by Mabuchi [6] using an approximate integral method.

Chen [7], Koh, Sparrow, and Hartnett [8], and Koh [9] considered almost simultaneously the effect of vapor drag. In this model, due to the no-slip condition at the interface of the vapor and the condensate, the motions of the vapor and condensate are considered

to be coupled. The solution of such a physical model requires a simultaneous solution of the flow fields in the vapor and liquid regions. The above investigators found that the effect of vapor drag on the heat transfer is quite small for large values of Prandtl number (Pr = 1 or greater). For fluids with small Prandtl number (usually liquid metals), vapor drag may cause a substantial reduction of the heat transfer rate. The reduction increases with increasing values of the parameter $C_{p\ell}\left(\frac{T_s - T_w}{\lambda}\right)$.

All the analyses so far reviewed were based on the assumption that the surface temperature of the film is equal to the saturation temperature of the vapor. These theories have adequately described the condensation process of steam or organic vapors, but the same thing can not be said for metal vapors.

Recently the use of liquid metal in heat transfer systems became popular in the field of nuclear and spacecraft engineering. The advantage of using liquid metal is its low vapor pressure compared to that of steam and organic vapors at the same temperature. This fact permits the use of light weight design for high temperature heat transfer systems.

The general observation of the condensation of metal vapors has been that the measured values of heat transfer rate fall far below the predictions of Nusselt's classical theory or the predictions of more recent modifications to that theory. Data of Misra and Bonilla [10] on condensing sodium and mercury vapors up to atomospheric pressure indicated that the film condensation heat transfer coefficients of mercury and sodium vapors are roughly 5%

to 15% of the value predicted by Nusselt's theory. Data of Cohn [11] on condensing mercury and cadmium vapors indicated that heat transfer coefficients for condensing metal vapors are about 1% to 15% of the coefficients deduced from Nusselt's theory. Similarly, discrepancies between Nusselt's classical theory and experimental data are shown in the recent data of Sukhatme and Rohsenow [12] for film condensation of mercury. Sukhatme measured condensate film thickness by gamma attenuation and found that the results agreed approximately with Nusselt's theory with an assumed temperature on the film surface. He also found that the condensing heat transfer coefficient increases with increasing vapor pressure, while the addition of a noncondensible gas to the system might cause a decrease in heat transfer coefficient with increasing vapor pressure. Based upon these findings, Sukhatme concluded that previous data for film condensation of metal vapors contain errors due to the presence of noncondensible gases.

Nusselt's theory and its refinements do not offer a satisfactory explanation of the condensation of metal vapors, but there remains one more assumption of Nusselt's theory to be examined; namely, that the surface temperature of the film is equal to the saturation temperature of the vapor. If the film surface temperature were much lower than the vapor temperature, the low heat transfer coefficient could be explained. The kinetic theory of condensation predicts implicitly a temperature jump at the liquid-vapor interface. Hence, the theory has been constantly used in explaining the condensation of metal vapors.

The classical model of kinetic theory of condensation was proposed by Hertz [13]. He considered a vapor at pressure P_v and temperature T_v condensing on a liquid whose surface temperature is T_s corresponding to a saturation pressure P_s. If it is assumed that the vapor has a Maxwellian velocity distribution, the molecular flux by weight can be calculated in both directions. These fluxes are

$$\left(\frac{W}{A}\right)_i = P_i\sqrt{\frac{M}{2\pi R T_i}} \qquad (i = v, s) \tag{1.2}$$

where $\left(\frac{W}{A}\right)_s$ represents the absolute rate of evaporation and $\left(\frac{W}{A}\right)_v$ represents the absolute rate of condensation. If these two fluxes are not equal, condensation or evaporation is occurring. It is possible that not all the molecules striking the liquid surface actually condense and a condensation coefficient σ_c is then introduced to account for this. An evaporation coefficient σ_e may be defined in a similar way as the fraction of the absolute evaporating flux which actually evaporates. The expression for the net rate of condensation is then given by

$$\left(\frac{W}{A}\right)_{net} = \sigma_c P_v\sqrt{\frac{M}{2\pi R T_v}} - \sigma_e P_s\sqrt{\frac{M}{2\pi R T_s}} \tag{1.3}$$

The value of σ_e may approach unity when evaporation is taking place in a high vacuum, but when condensation is taking place, it is evident that σ_e could have values much less than unity due to

the interference of the condensing molecules with the evaporating molecules. In the absence of specific knowledge about the evaporation coefficient, certain assumptions have to be made. The assumptions which have been used most often in the study of experimental data of condensation are that either $\sigma_e = 1$ or $\sigma_e = \sigma_c$. As should be noted, $\sigma_e = \sigma_c$ only makes sense in equilibrium and there is no physical reason why this should hold away from equilibrium.

The first improvement in Hertz's formula was made by Schrage [14] and later Kucherov and Rikenglaz [15]. They derived a correction to account for the net motion due to a steady state condensation. By including the mean velocity in the distribution function for vapor moving toward the liquid surface, a correction Γ was found in calculating the absolute rate of condensation. The expression for the net rate of condensation due to Schrage is given by

$$\left(\frac{W}{A}\right)_{net} = \sigma_c \Gamma P_v \sqrt{\frac{M}{2\pi R T_v}} - \sigma_e P_s \sqrt{\frac{M}{2\pi R T_s}} \tag{1.4}$$

where

$$\Gamma = e^{-\phi^2} + \phi \pi^{1/2} (1 + erf\, \phi) \tag{1.5}$$

and

$$\phi = \frac{\left(\frac{W}{A}\right)_{net}}{\rho_v \left(\frac{2RT_v}{M}\right)^{1/2}} \tag{1.6}$$

In Hertz's or Schrage's model, they apparently assumed that bulk vapor conditions prevail up to the vapor-liquid interface, and predicted a temperature jump in one mean free path from the liquid surface.

Labuntsov [16] and later Patton and Springer [17] removed this unrealistic assumption using the double Maxwell distribution function along with Lees' moment method. They first considered a case of two surfaces - evaporating and condensing - as boundaries where the temperature, velocity, and number density of evaporation are specified. Using the same technique, Patton and Springer modified Hertz's model and the result was given by

$$\left(\frac{W}{A}\right)_{net} = -\frac{\sqrt{2\pi R T_v}}{2\pi}\, \rho_v \left\{ \frac{\frac{1}{2}\frac{\Delta T}{T_v}\left(\frac{1}{1+4/5\,K_n}+\frac{\sigma_e}{\sigma_c}-1\right)-\frac{\Delta P}{P_v}\frac{\sigma_e}{\sigma_c}-1+\frac{\sigma_e}{\sigma_c}}{\frac{1}{\sigma_c}-\frac{1}{2}+\frac{1}{2+8/5\,K_n}} \right\} \quad (1.7)$$

where $\Delta T = T_v - T_s$ and $\Delta P = P_v - P_s$, while K_n is the Knudsen number defined as the ratio of mean free path to a convenient characteristic length.

Schrage's formula was used by Sukhatme, Barry [18], Minkowycz [19] and many others in analyzing their experimental data of condensing vapors, while the Patton-Springer formula was used recently by Sartor [20]. They found, in general, that the theory fails to explain the results of experiments. They assumed either $\sigma_e = 1$ or $\sigma_e = \sigma_c$ and expected to get a constant value of σ_c. Unfortunately, for $\sigma_e = 1$, σ_c can range from .04 up to .45 for steam and up to 1 for alkali metal vapors.

The inadequacy of Nusselt's theory and the unsatisfactory explanation of the temperature drop at the liquid-vapor interface from the kinetic theory of condensation motivated the present investigation. This investigation has been undertaken to provide an explanation of the temperature drop near the liquid-vapor interface in the condensation of low pressure metal vapors. The physical model studied is that of laminar film condensation of vapor on an isothermal vertical surface. A solution has been obtained which permits the prediction of condensation of pure vapors or mixtures of a vapor and noncondensible gases. It has been found that a large temperature drop can exist near the interface in a narrow region whose thickness is proportional to but much larger than the mean free path and inversely proportional to the mean Mach number of the condensing vapor.

Details of film condensation of a pure vapor on an isothermal vertical flat plate have been carried out in Section II. Fairly good agreement between the theory and Sartor's data for condensation of one-dimensional flow of rubidium vapor has been obtained. However, if one uses this theory, there is still rather poor agreement with Sukhatme's data for condensation of mercury vapor on a finger type condenser. The poor agreement is probably due to the presence of noncondensible gases and to the isentropic expansion of the vapor itself. This vapor expansion was not present in Sartor's one-dimensional flow. In Section III, we have extended the theory for pure vapor to include the presence of noncondensible gases. As expected, the presence of noncondensible gases plays a

decisive role in retarding the condensation rate of low pressure metal vapors. In Section IV, we have included the additional temperature drop due to the expansion of the vapor. In some situations, the temperature drop due to the expansion of the vapor may be more significant than the interfacial temperature drop. The final result is good agreement between theory and experiments.

II. FILM CONDENSATION OF A PURE VAPOR ON AN ISOTHERMAL VERTICAL FLAT PLATE

2.1 Discussion of the Analytical Model

The vapor flow field for the present problem of film condensation on an isothermal vertical flat plate can be divided into three regions as shown in Fig. 1. In region I, the y-component of the mean velocity of the vapor at infinity is much greater than the maximum value of the x-component of velocity; namely, the downward velocity at the liquid-vapor interface. In this case the dynamics of the vapor flow normal to the plate is important and can not be neglected. In region II, the maximum values of the two components of velocity are about the same order of magnitude. In region III, the liquid film plays the important part and the dynamics of the vapor can be completely neglected.

Under conditions of (a) large value of latent heat, (b) long length of condensing plate, and (c) high vapor density, region III will dominate and the temperature change in the vapor may be neglected. These conditions are usually met in condensing steam and organic vapor systems and explain why Nusselt's theory works. On the other hand, the condensation of low pressure metal vapor generally occurs under the following conditions: (a) a smaller value of latent heat, (b) short length of condensing plate, and (c) low vapor density. Under these conditions, vapor flow is important. The corresponding temperature drop in the vapor can not be neglected.

If a temperature at the liquid-vapor interface is assumed, the liquid film and the vapor can be treated independently. The

former is treated as a liquid boundary layer, while the latter is treated as a one-dimensional vapor flow. However, the two problems are really coupled since the temperature is assumed to be continuous at the interface. A kinetic theory argument is necessary to determine the condensation rate and hence the interface temperature.

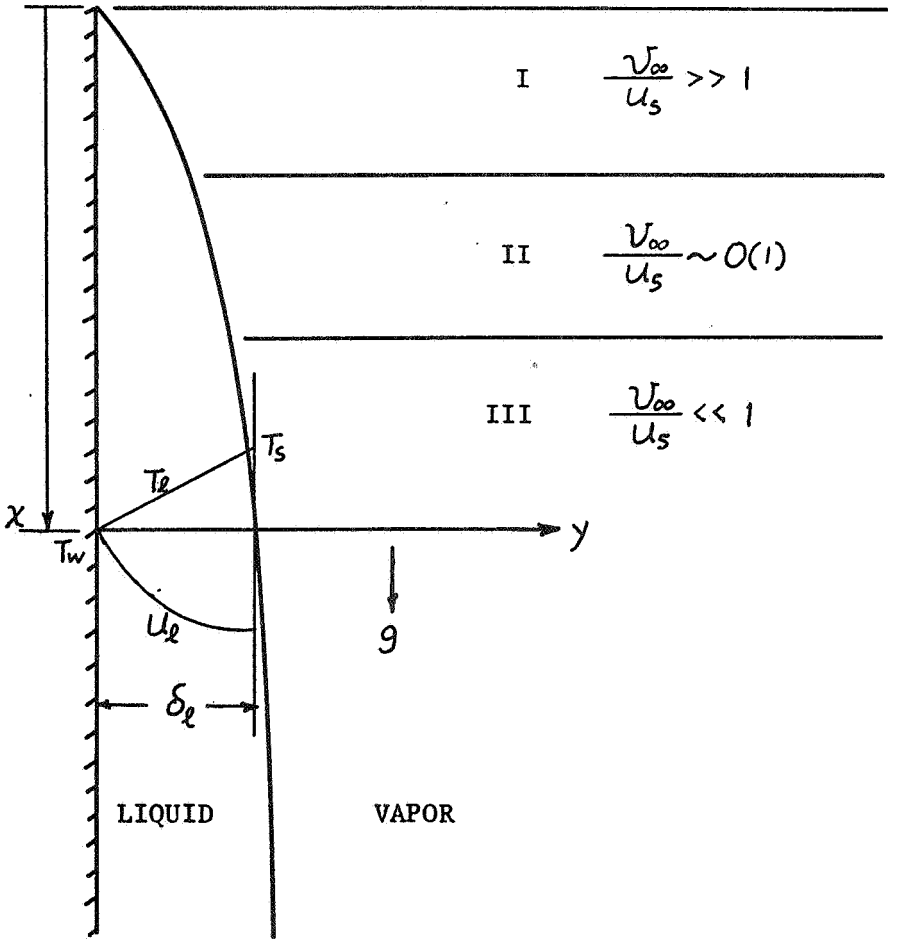

Figure 1. Schematic of film condensation

2.2 Liquid Film

The specific problem that will be analyzed includes the following assumptions: (a) the surface temperature of the liquid film is constant, (b) the condensate flow is laminar, (c) the fluid properties are constant, (d) momentum changes through the condensate are negligible and the viscous force balances the body force, (e) the vapor drag at the interface is neglected, and (f) the temperature distribution in the liquid film is linear, which becomes exact for low Prandtl number. A schematic representation of the physical model and coordinate system has been shown in Fig. 1.

With these approximations, the equations expressing conservation of mass, momentum, and energy in the liquid film are:

Continuity:

$$\frac{\partial u_\ell}{\partial x} + \frac{\partial v_\ell}{\partial y} = 0 \tag{2.2.1}$$

Momentum:

$$g\rho_\ell + \mu_\ell \frac{\partial^2 u_\ell}{\partial y^2} = 0 \tag{2.2.2}$$

Energy:

$$\frac{\partial}{\partial y}\left(k_\ell \frac{\partial T_\ell}{\partial y}\right) = 0 \tag{2.2.3}$$

The boundary conditions appropriate to the liquid film are:

Wall conditions ($y = o$)

$$u_\ell = v_\ell = 0 \quad , \qquad T_\ell = T_w \tag{2.2.4}$$

Interface conditions ($y = \delta_\ell$)

$$\frac{\partial u_\ell}{\partial y} = 0 \quad , \qquad T_\ell = T_s \tag{2.2.5}$$

All symbols are defined in the list of symbols and further elaboration is given only when necessary.

Equations (2.2.2) and (2.2.3) can be solved along with the boundary conditions (2.2.4) and (2.2.5). The solutions are

$$u_\ell = \frac{g \rho_\ell}{2 \mu_\ell} \delta_\ell^2 \left(2 \frac{y}{\delta_\ell} - \frac{y^2}{\delta_\ell^2} \right) \tag{2.2.6}$$

$$T_\ell = T_w + (T_s - T_w) \frac{y}{\delta_\ell} \tag{2.2.7}$$

v_ℓ has been omitted since it is not important in the problem.

The thickness distribution (δ_ℓ) of liquid film may be found explicitly if one assumes that all the heat flow through the liquid is generated by condensation of vapor at the outer edge of the liquid film. The heat flow dQ through the liquid with the height dx and unit dimension in the horizontal direction along the wall is

$$dQ = \frac{K_\ell}{\delta_\ell} (T_s - T_w) \, dx \tag{2.2.8}$$

The mass of liquid flowing through this cross section at x is

$$G = \int_0^{\delta_\ell} \rho_\ell u_\ell \, dy \tag{2.2.9}$$

Integration gives

$$G = \frac{g \rho_\ell^2}{3 \mu_\ell} \delta_\ell^3 \tag{2.2.10}$$

At a distance dx in the downward direction, the mass flow is greater by the amount

$$dG = \frac{g \rho_\ell^2}{\mu_\ell} \delta_\ell^2 \frac{d\delta_\ell}{dx} dx \tag{2.2.11}$$

This amount must be generated by condensation of vapor. With the equation $dQ = \lambda \, dG$, in which λ is the latent heat of vaporization, there is obtained from equation (2.2.8)

$$dG = \frac{K_\ell}{\lambda \delta_\ell} (T_s - T_w) \, dx \tag{2.2.12}$$

By equating (2.2.11) and (2.2.12), the formula

$$\delta_\ell^3 \frac{d\delta_\ell}{dx} = \frac{\mu_\ell K_\ell}{\lambda g \rho_\ell^2} (T_s - T_w) \tag{2.2.13}$$

is obtained. Integration of equation (2.2.13) with the condition of vanishing thickness at the leading edge gives

$$\delta_\ell = \left[\frac{4 \nu_\ell K_\ell (T_s - T_w)}{\lambda g \rho_\ell} \; x \right]^{\frac{1}{4}} \tag{2.2.14}$$

For a given length of condensing plate, an effective film thickness $(\delta_\ell)_e$ and a mean mass flux per unit area $\bar{G}$ are defined

$$\bar{G} = \frac{1}{L} \int_0^L G \, dx \tag{2.2.15}$$

$$\bar{G} = \frac{K_\ell}{(\delta_\ell)_e} (T_s - T_w) \tag{2.2.16}$$

where

$$(\delta_\ell)_e = \frac{3}{4} \left[\frac{4 \nu_\ell K_\ell L (T_s - T_w)}{\lambda g \rho_\ell} \right]^{\frac{1}{4}} \tag{2.2.17}$$

The mean heat transfer rate of condensation per unit area is calculated by the formula

$$\bar{Q} = \lambda \bar{G} \tag{2.2.18}$$

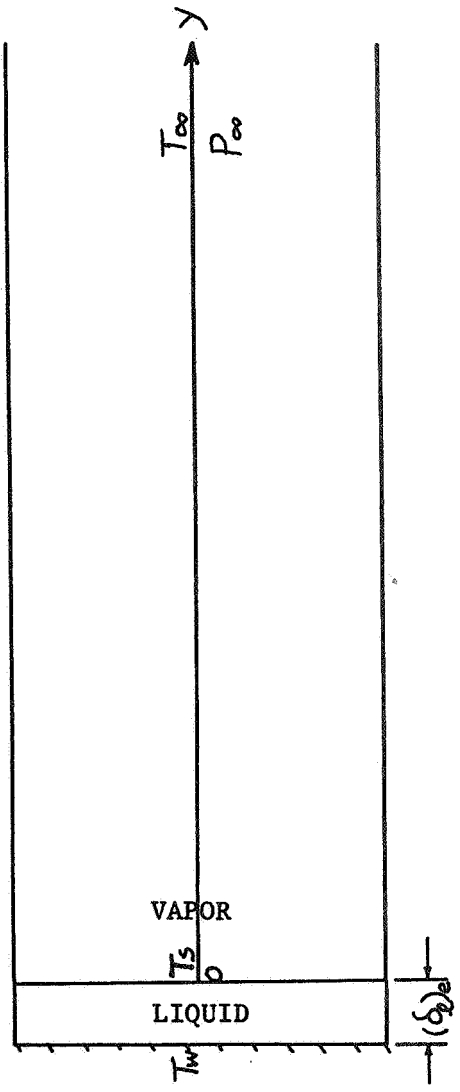

Figure 2. Schematic of one-dimensional vapor flow

2.3 Vapor Flow

The vapor will be treated approximately as a one-dimensional flow. The general analysis may be simplified by use of the following assumptions: (a) the properties of the vapor are constant, (b) the total temperature drop in the vapor is much smaller than the absolute bulk temperature, although it may be much greater than the temperature drop across the liquid film, (c) the Mach number of mean vapor flow is very small, and (d) the vapor obeys the perfect gas law. The simplified model and coordinate system is sketched in Fig. 2.

The governing equations of the vapor flow are:

Continuity:

$$\frac{d}{dy}(\rho v) = 0 \tag{2.3.1}$$

Momentum:

$$\rho v \frac{dv}{dy} = -\frac{dp}{dy} + \frac{4}{3}\mu \frac{d^2 v}{dy^2} \tag{2.3.2}$$

Energy:

$$\rho v C_p \frac{dT}{dy} = K \frac{d^2 T}{dy^2} + v \frac{dp}{dy} + \frac{4}{3}\mu \left(\frac{dv}{dy}\right)^2 \tag{2.3.3}$$

State:

$$p = \rho R_M T \tag{2.3.4}$$

The temperature and pressure at infinity and the temperature on the wall are usually given as boundary conditions, while the velocity at infinity is found from the mean mass flux divided by the vapor density at infinity. The appropriate boundary conditions for the vapor are:

Bulk vapor conditions ($y \longrightarrow \infty$)

$$T = T_\infty \ , \qquad P = P_\infty \ , \qquad v = v_\infty = -\frac{\bar{G}}{\rho_\infty} \tag{2.3.5}$$

Interface condition ($y = 0$)

$$T = T_s \tag{2.3.6}$$

Integration of equations (2.3.1) and (2.3.2) gives

$$\rho v = \rho_\infty v_\infty = -\bar{G} \tag{2.3.7}$$

$$P + \rho v^2 = \frac{4}{3}\mu \frac{dv}{dy} + C_1 \tag{2.3.8}$$

where

$$C_1 = -\bar{G}\left(\frac{P_\infty}{\rho_\infty v_\infty} + v_\infty \right) \tag{2.3.9}$$

By multiplying the momentum equation by v , adding the result to the energy equation, and integrating, one obtains

$$\rho v\left(C_p T + \frac{v^2}{2}\right) = K\frac{dT}{dy} + \frac{4}{3}\mu v\frac{dv}{dy} + C_2 \qquad (2.3.10)$$

where

$$C_2 = -\bar{G}\left(C_p T_\infty + \frac{v_\infty^2}{2}\right) \qquad (2.3.11)$$

Denoting $\frac{\mu C_p}{K}$ by Prandtl number P_r and replacing C_p by $\frac{\gamma}{\gamma-1}R$ in which γ is the ratio of specific heats, equations (2.3.8) and (2.3.10) may be rearranged in the following forms

$$-\frac{4}{3}\frac{\mu}{\bar{G}}\frac{dv}{dy} = v + \frac{RT}{v} + \frac{C_1}{\bar{G}} \qquad (2.3.12)$$

and

$$-\frac{4}{3}\frac{\mu}{\bar{G}}\frac{dT}{dy}\left(\frac{3}{4}\frac{\gamma}{\gamma-1}\frac{R}{P_r}\right) = \frac{RT}{\gamma-1} - \frac{v^2}{2} - \frac{C_1}{\bar{G}}v - \frac{C_2}{\bar{G}} \qquad (2.3.13)$$

These are a set of nonlinear differential equations. For small deviations about the singular point at infinity, the system can be linearized.

Let

$$T = T_\infty + T' \qquad (2.3.14)$$

$$v = v_\infty + v' \qquad (2.3.15)$$

By substituting these relations into equations (2.3.12) and (2.3.13) and dropping second order terms, one obtains the linearized system,

$$-\frac{4}{3}\frac{\mu}{\bar{G}}\frac{dv'}{dy} = 2v' + \frac{c_1}{\bar{G}}\frac{v'}{v_\infty} + R\frac{T'}{v_\infty} \tag{2.3.16}$$

$$-\frac{4}{3}\frac{\mu}{\bar{G}}\frac{dT'}{dy}\left(\frac{\gamma}{\gamma-1}\frac{3}{4}\frac{R}{P_r}\right) = \frac{R}{\gamma-1}T' - v_\infty v' - \frac{c_1}{\bar{G}}v' \tag{2.3.17}$$

The solution may be found by assuming

$$T' = A e^{-\alpha\frac{3}{4}\frac{\bar{G}}{\mu}y} \tag{2.3.18}$$

$$v' = B e^{-\alpha\frac{3}{4}\frac{\bar{G}}{\mu}y} \tag{2.3.19}$$

which, after rearrangements of equations (2.3.16) and (2.3.17), lead to the system

$$(\gamma\alpha - \frac{4}{3}P_r)RA - \frac{4}{3}P_r\frac{\gamma-1}{\gamma M_\infty^2}v_\infty B = 0 \tag{2.3.20}$$

$$RA + \left[(1-\alpha) - \frac{1}{\gamma M_\infty^2}\right]v_\infty B = 0 \tag{2.3.21}$$

where A, B and α are arbitrary constants and

$$M_\infty^2 = \frac{\rho_\infty v_\infty^2}{\gamma P_\infty} \tag{2.3.22}$$

To have a nontrivial solution, the determinant of coefficients of A and B must vanish.

$$\left(\frac{4}{3}P_r - 1\alpha\right)(1-\alpha)M_\infty^2 - \frac{4}{3}P_r + \alpha = 0 \qquad (2.3.23)$$

which may be written

$$1M_\infty^2\alpha^2 - \left(1M_\infty^2 + \frac{4}{3}P_r M_\infty^2 - 1\right)\alpha + \frac{4}{3}P_r(M_\infty^2 - 1) = 0 \qquad (2.3.24)$$

The roots of this equation are

$$\alpha = \frac{1}{2}\left(1 + \frac{4}{3}\frac{P_r}{1} - \frac{1}{1M_\infty^2}\right) \pm \frac{\sqrt{\left(1M_\infty^2 - \frac{4}{3}P_r M_\infty^2 - 1\right)^2 + \frac{16}{3}P_r(1-1)M_\infty^2}}{21M_\infty^2} \qquad (2.3.25)$$

The root with plus sign is necessary in the present problem. The root with minus sign is rejected, since it is negative for Mach number less than unity.

The solution for the condensation of metal vapor when the Prandtl number is two-thirds is presented here. The appropriate root is obtained from equation (2.3.25) and is

$$\alpha = \frac{1}{2}\left(1 + \frac{8}{9}\frac{1}{1} - \frac{1}{1M_\infty^2}\right) + \frac{1}{2}\sqrt{\left(\frac{1}{1M_\infty^2} + \frac{8}{9}\frac{1}{1} - 1\right)^2 + \frac{32}{9}\left(\frac{1-1}{1}\right)\frac{1}{1M_\infty^2}} \qquad (2.3.26)$$

In the limiting case ($M_\infty \longrightarrow 0$), there is obtained from equation (2.3.26)

$$\alpha \cong \frac{8}{9} \tag{2.3.27}$$

and from equation (2.3.20) or (2.3.21)

$$\frac{A}{B} \cong \frac{T_\infty}{U_\infty} \tag{2.3.28}$$

By substituting these results into equations (2.3.18) and (2.3.19) and applying the appropriate boundary conditions, one obtains from equations (2.3.14) and (2.3.15) the results that

$$T \cong T_\infty - \left(\frac{T_\infty - T_s}{T_\infty}\right) T_\infty \, e^{-\frac{2}{3}\frac{\bar{G}}{\mu} y} \tag{2.3.29}$$

$$U \cong U_\infty - \left(\frac{T_\infty - T_s}{T_\infty}\right) U_\infty \, e^{-\frac{2}{3}\frac{\bar{G}}{\mu} y} \tag{2.3.30}$$

The density may be obtained from equation (2.3.7) and is

$$\rho \cong \rho_\infty + \left(\frac{T_\infty - T_s}{T_\infty}\right) \rho_\infty \, e^{-\frac{2}{3}\frac{\bar{G}}{\mu} y} \tag{2.3.31}$$

The pressure may be obtained directly from the equation of state and is

$$P \cong P_\infty - \left(\frac{T_\infty - T_s}{T_\infty}\right)^2 P_\infty \left[e^{-\frac{2}{3}\frac{\bar{G}}{\mu} y}\right]^2 \tag{2.3.32}$$

In this limit ($M_{\infty} \rightarrow 0$), the linearized solution indicates that the temperature and velocity vary exponentially in a very thin layer near the interface, while the pressure is approximately constant (if $\frac{T_{\infty} - T_s}{T_{\infty}} << 1$). For a saturated bulk vapor, the vapor at the interface is therefore in a supersaturated condition.

2.4 Distribution Function

The previous analysis does not permit the calculation of the temperature T_s at the interface. However, this temperature can be determined if one constructs a consistent distribution function which correctly describes the average or macroscopic behavior of the vapor at the interface.

A distribution function is assumed for those particles on the vapor side at the plane which is parallel to and located very close to the interface. The assumed distribution function consists of three parts and is written

$$f = f_1 + f_2 + f_3 \tag{2.4.1}$$

f_1 represents particles leaving the liquid with zero drift velocity. f_2 represents particles entering the liquid with a drift velocity $\bar{v}_d$. f_3 represents particles not entering the liquid but moving over the condensing surface. Since the condensing surface can serve as an energy absorber, the energy normal to the surface may be absorbed and transferred away through the liquid. Hence, for particles of the third kind, the thermal energy normal to the condensing surface may be much smaller than the mean thermal energy.

Denoting by T_Δ the temperature of particles of the third kind normal to the condensing surface, this assumption can be written as

$$\frac{T_\Delta}{T_s} << 1 \quad or \quad \frac{T_\Delta}{T_s} \longrightarrow 0 \tag{2.4.2}$$

The forms of f_1 , f_2 and f_3 are assumed

$$f_1 = n_s \left(\frac{m}{2\pi k T_s}\right)^{3/2} exp\left(-m \frac{U^2+V^2+W^2}{2kT_s}\right) \tag{2.4.3}$$

$$f_2 = n_s \left(\frac{m}{2\pi k T_s}\right)^{3/2} exp\left[-m \frac{U^2+(V-\bar{v}_d)^2+W^2}{2kT_s}\right] \tag{2.4.4}$$

$$f_3 = n_\Delta \left(\frac{m}{2\pi k T_s}\right) exp\left(-m\frac{U^2+W^2}{2kT_s}\right)\left(\frac{m}{2\pi k T_\Delta}\right)^{1/2} exp\left(-m\frac{V^2}{2kT_\Delta}\right) \tag{2.4.5}$$

If the mean drift velocity of particles of the second kind is much smaller than the mean thermal speed, equation (2.4.4) may be simplified to

$$f_2 \cong \left(1+\frac{2\bar{v}_d}{a_s^2}V\right) f_1 \tag{2.4.6}$$

where

$$a_s^2 = \frac{2kT_s}{m} \tag{2.4.7}$$

The macroscopic properties of the vapor at the interface are calculated from the following definitions:

Temperature:

$$\frac{3}{2} k T_i = \frac{\int_{-\infty}^{\infty}\int\int \frac{1}{2} m C^2 f \, dU dV dW}{\int_{-\infty}^{\infty}\int\int f \, dU dV dW} \tag{2.4.8}$$

Density:

$$\rho_i = \int_{-\infty}^{\infty}\int\int m f \, dU \, dV dW \tag{2.4.9}$$

Velocity:

$$U_i = \frac{\int_{-\infty}^{\infty}\int\int m V f \, dU dV dW}{\int_{-\infty}^{\infty}\int\int m f \, dU dV dW} \tag{2.4.10}$$

which may be written as

$$-\bar{G} = \int_{-\infty}^{\infty}\int\int m V f \, dU dV dW \tag{2.4.11}$$

The interface conditions are chosen to be those of the previous analysis in section (2-3); namely $T_i = T_s$, $P_i \cong P_\infty$, and $\rho_i \cong \frac{P_\infty}{R_M T_s}$.

Direct integration of equations (2.4.8), (2.4.9) and (2.4.11) yields

$$1 = \frac{\rho_s\left(1 - \frac{4}{3}\frac{\bar{v}_d}{\pi^{1/2} a_s}\right) + \frac{2}{3}\rho_\Delta + \frac{1}{3}\rho_\Delta\left(\frac{T_\Delta}{T_s}\right)}{\rho_s\left(1 - \frac{\bar{v}_d}{\pi^{1/2} a_s}\right) + \rho_\Delta} \tag{2.4.12}$$

$$\frac{p_\infty}{R_M T_s} = \rho_s\left(1 - \frac{\bar{v}_d}{\pi^{1/2} a_s}\right) + \rho_\Delta \tag{2.4.13}$$

$$\bar{G} = -\rho_s \frac{\bar{v}_d}{2} \tag{2.4.14}$$

where ρ_s is the saturation density at temperature T_s, while ρ_Δ is the density of particles of the third kind.

From equation (2.4.12), one obtains

$$\rho_\Delta = -\rho_s \frac{\bar{v}_d}{\pi^{1/2} a_s}\left(\frac{1}{1 - \frac{T_\Delta}{T_s}}\right) \tag{2.4.15}$$

By substituting ρ_Δ from equation (2.4.15) into equation (2.4.13) and making use of equation (2.4.14), one obtains the important formula

$$p_\infty - p_s = \frac{\bar{G}}{\pi}\left(2\pi R_M T_s\right)^{1/2}\left(2 + \frac{\frac{T_\Delta}{T_s}}{1 - \frac{T_\Delta}{T_s}}\right) \tag{2.4.16}$$

which, when rewritten for the case of $\frac{T_\Delta}{T_s} \longrightarrow 0$,

$$P_\infty - P_s = \frac{2}{\pi} \bar{G} \left(2\pi R_M T_s\right)^{\frac{1}{2}} \tag{2.4.17}$$

where P_s is a given function of T_s , while $\bar{G}$ is defined by equation (2.2.16). Then the temperature T_s can be determined by equation (2.4.17).

With the present approximation for the distribution function, an interesting coefficient σ_H may be defined which resembles the usual condensation coefficient; namely, σ_H is the fraction of the total number density of particles of the second and third kind that will actually condense, i.e.,

$$\sigma_H = \frac{\iiint_{-\infty}^{\infty}\int_{-\infty}^{0} f_2 \, dU dV dW}{\iiint_{-\infty}^{\infty}\int_{-\infty}^{0} f_2 \, dU dV dW + \iiint_{-\infty}^{\infty} f_3 \, dU dV dW} \tag{2.4.18}$$

By integrating and making use of previous results, one obtains from equation (2.4.18)

$$\sigma_H = 1 - \frac{\frac{P_\infty - P_s}{P_\infty}}{1 + \frac{P_\infty - P_s}{P_\infty}} \tag{2.4.19}$$

In the present problem, σ_H has values between 0.5 and 1.0 and is shown in Fig. 3. When the condensation rate is zero, σ_H is unity and starts decreasing as the condensation rate increases.

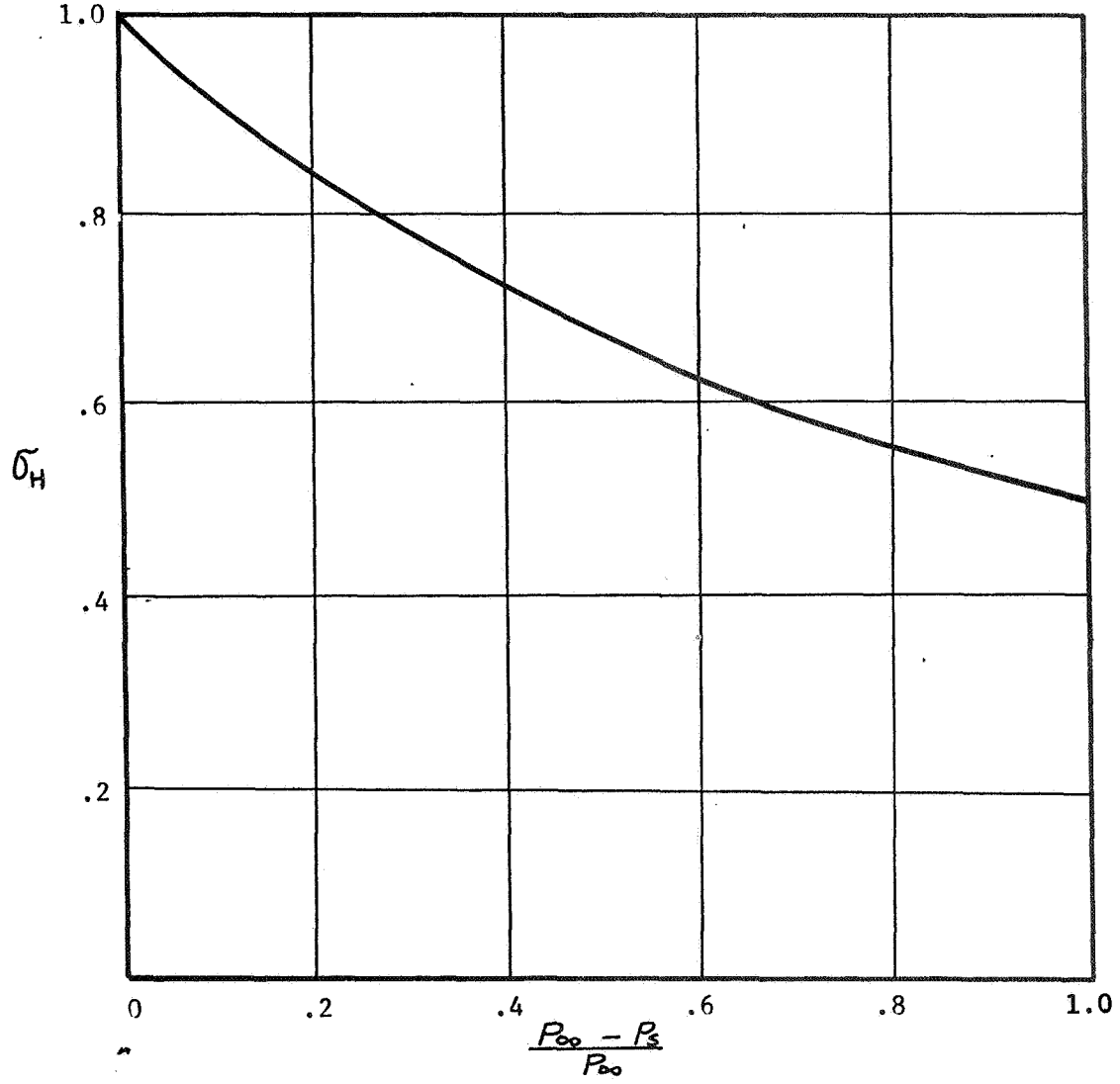

Figure 3. σ_H versus $\frac{P_\infty - P_s}{P_\infty}$

2.5 Results of Calculations

The results of calculations based on the present theory are presented as curves of heat transfer rate per unit area ($\bar{Q}$) versus the total temperature drop ($T_\infty - T_w$) for different values of vapor pressure P_∞ .

For a fixed vapor pressure P_∞ , one first calculates the mass flux $\bar{G}$ from equation (2.4.17) for any value of T_s , and then, from equations (2.2.16) and (2.2.17), calculates the temperature drop across the liquid film. The heat flux per unit area $\bar{Q}$ can be calculated from equation (2.2.18), while the total temperature drop is the sum of the temperature drop in the vapor and in the liquid film. In practical cases, T_w is given and $\bar{G}$ and T_s can be obtained by trial and error.

Some analytical results for condensation of one dimensional Rubidium vapor are shown in Fig. 4. The physical properties of Rubidium are taken from reference [21] as follows:

K_ℓ = 23 BTU/hr-ft-°F

ρ_ℓ = 92 lbm/ft^3

$C_{p\ell}$ = .0913 BTU/lbm-°F

μ_ℓ = 60 lbm/ft-hr

λ = 381 BTU/lbm

M = 85.5 lbm/mole

The saturation pressure as a function of temperature (shown in Figure 5)

The thickness of the liquid layer is chosen to be 0.12 inches which has been used in Sartor's experiment.

In Fig. 4, curves 1 and 2 are for the highest and lowest vapor pressures in Sartor's data. Curves 3 and 4 are for much lower pressures to show the dependence of heat transfer rate on the vapor pressure. As can be seen, lower vapor pressures give lower heat transfer rates.

It can be shown that the interfacial region across which the temperature drop inside the vapor occurs is very thin. The Mach number in Sartor's experiments with Rubidium varies from .002 to .005. The thickness of the interfacial region is about 500 to 1000 mean free paths of rubidium vapor, or of the order of 5×10^{-5} inches. This confirms Sartor's conclusion that there is a rapid temperature change near the liquid-vapor interface.

As a comparison with Nusselt's theory, the ratio of average heat transfer coefficient of the present theory to Nusselt's theory is plotted againt the parameter $C_{pl}\left(\frac{T_\infty - T_w}{\lambda}\right)$ in Fig. 6. The general trend is that lower vapor pressure gives greater deviation from Nusselt's theory.

The agreement between Sartor's data and the theoretical prediction is good with the discrepancy between the two being less than ten percent, but more data in a much lower pressure range is needed to justify the theory. Some important experiments of condensation of metal vapors at lower pressures have been conducted on a finger type condenser. Available data shows heat flux is considerably smaller than the predictions from the present theory. The discrepancy may be due to the presence of noncondensible gases and to the isentropic expansion flow of the vapor itself. A study of the effect of the

presence of noncondensible gases is presented in Section III. In Section IV, the condensation of a metal vapor on a finger type condenser is discussed. The effects of noncondensible gases and of vapor expansion are included.

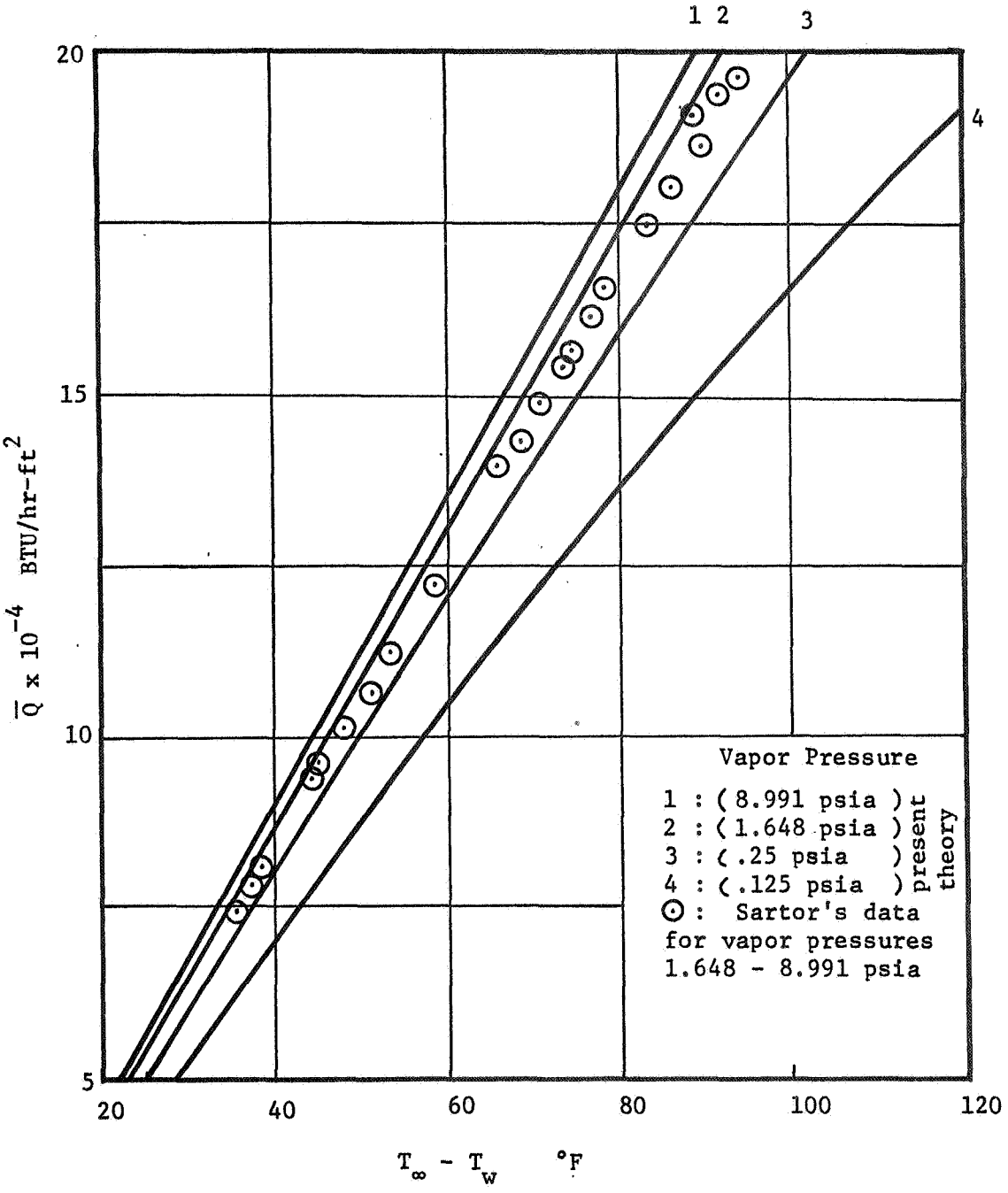

Figure 4. Comparison of present theory with experimental data (Rubidium)

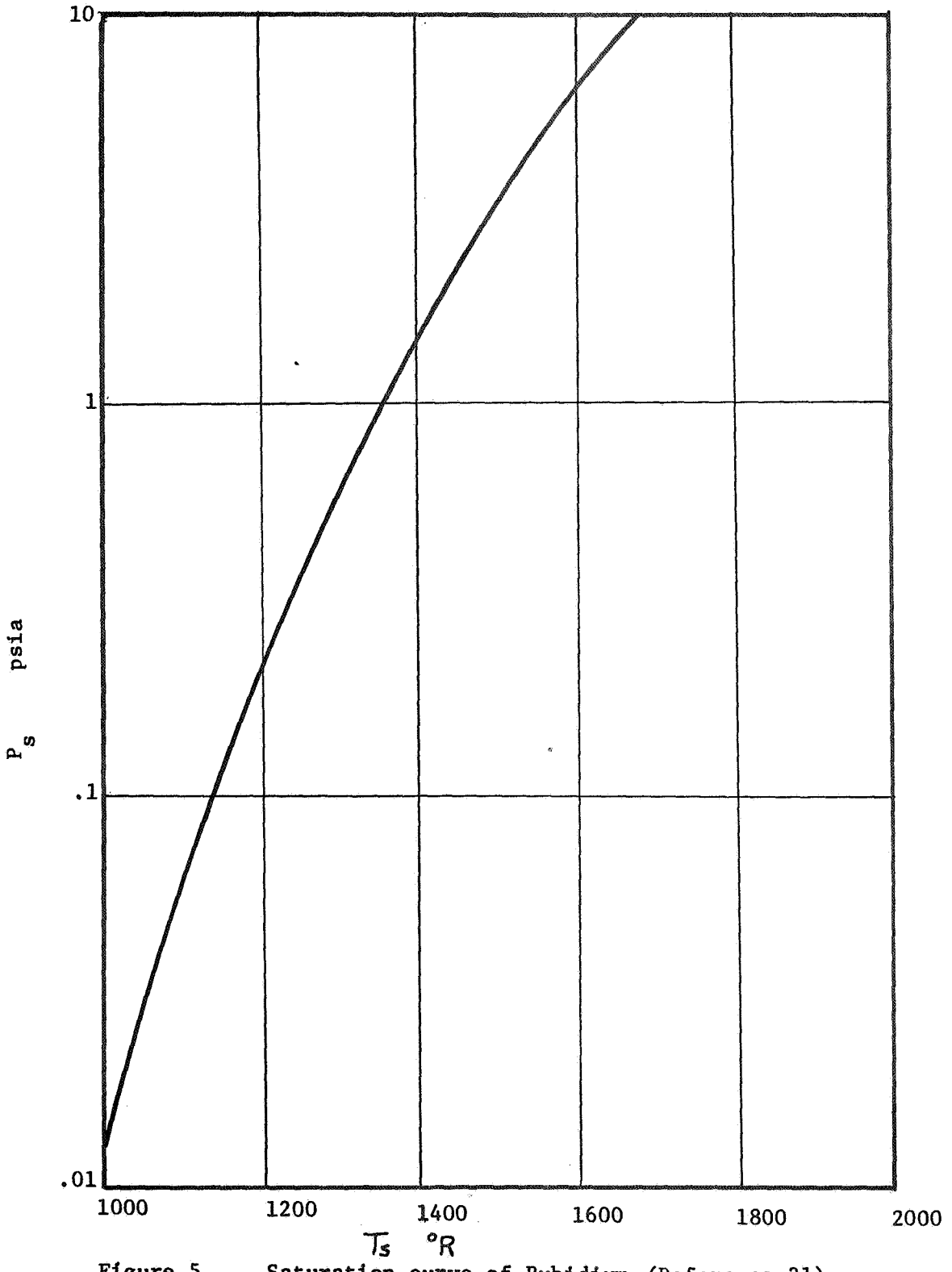

Figure 5. Saturation curve of Rubidium (Reference 21)

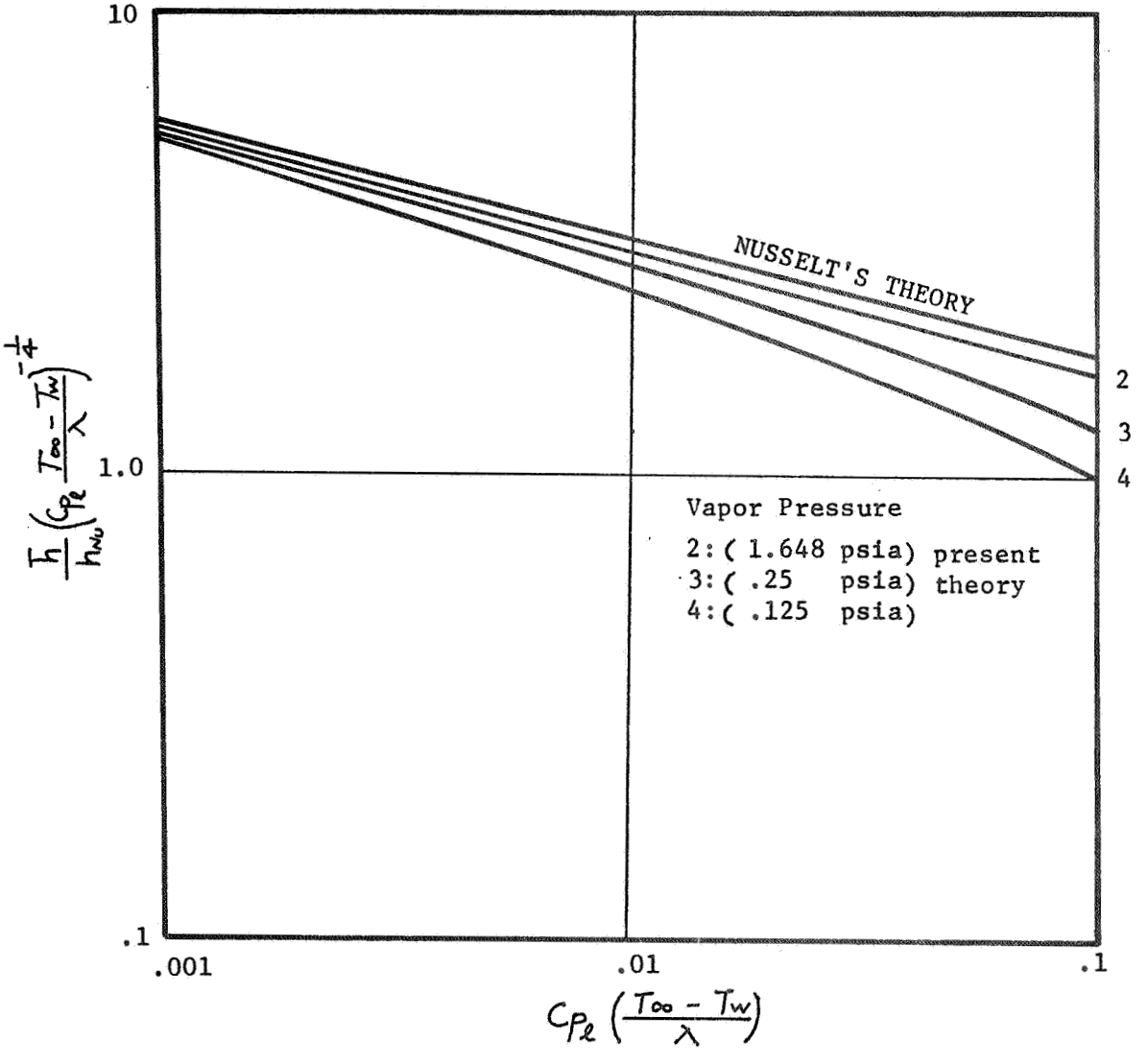

Figure 6. Comparison of present theory with Nusselt's theory (Rubidium)

III. CONSIDERATION OF THE PRESENCE OF NONCONDENSIBLE GASES

The following analysis is restricted to a system with only two components, namely a mixture of vapor and air. In practice, the amount of air is kept as low as possible and therefore the concentration of air may be assumed to be very small. The same physical model shown in Fig. 2 is used here. The governing equations for a mixture are as follows:

Continuity:

$$\frac{d}{dy}(\rho v) = 0 \tag{3.1}$$

Momentum:

$$\rho v \frac{dv}{dy} = -\frac{dP}{dy} + \frac{4}{3}\frac{d}{dy}\left[\mu \frac{dv}{dy}\right] \tag{3.2}$$

Energy:

$$\rho v C_p \frac{dT}{dy} = v\frac{dP}{dy} + \frac{d}{dy}\left[K \frac{dT}{dy}\right] + \frac{4}{3}\mu\left(\frac{dv}{dy}\right)^2 \tag{3.3}$$

State:

$$P = \rho R_M T \tag{3.4}$$

Diffusion:

$$\rho v W = \rho D_{12} \frac{dW}{dy} \tag{3.5}$$

The balance between mass convection and mass diffusion is represented by equation (3.5), in which W is the concentration or mass fraction of air and D_{12} is the diffusion coefficient of a mixture.

Subscripts 1 and 2 denote respectively the pure vapor and air. The properties of a mixture are calculated from the kinetic theory for a rigid spherical molecule [22, 23]. The results are expanded in a power series in W. Since W is very small, only the first order term is kept in the expansion.

Viscosity:

$$\mu \cong \mu_1 - \frac{M_1}{M_2}\left(\mu_1 \xi_{12} - \frac{\mu_2}{\xi_{21}}\right) W + \cdots \tag{3.6}$$

Conductivity:

$$K \cong K_1 - \frac{M_1}{M_2}\left(K_1 \xi_{12} - \frac{K_2}{\xi_{21}}\right) W + \cdots \tag{3.7}$$

Gas constant:

$$R_M = R_{M_1} - R_{M_1}\left(1 - \frac{M_1}{M_2}\right) W \tag{3.8}$$

Specific heat:

$$C_p = C_{p_1} + \left(C_{p_2} - C_{p_1}\right) W \tag{3.9}$$

Diffusion coefficient:

$$D_{12} = \frac{3}{8}\sqrt{\frac{\pi}{2}}\,\frac{kT}{P\pi}\,\frac{1}{\left(\frac{\sigma_1 + \sigma_2}{2}\right)^2}\left(\frac{M_1 + M_2}{M_1 M_2} RT\right)^{\frac{1}{2}} \tag{3.10}$$

where σ is the diameter of a molecule and

$$\varepsilon_{ij} = \left(\frac{\sigma_i + \sigma_j}{2\sigma_i}\right)^2 \left(\frac{1 + \frac{M_i}{M_j}}{2}\right)^{\frac{1}{2}} \qquad (i = 1, 2;\ j = 1, 2) \qquad (3.11)$$

In these equations, all the properties will be evaluated at the vapor temperature T_∞ .

Using the method of regular perturbation, one sets

$$P \cong P^{(0)} + w_i P^{(1)} + w_i^2 P^{(2)} + \cdots \qquad (3.12)$$

$$\rho \cong \rho^{(0)} + w_i \rho^{(1)} + w_i^2 \rho^{(2)} + \cdots \qquad (3.13)$$

$$T \cong T^{(0)} + w_i T^{(1)} + w_i^2 T^{(2)} + \cdots \qquad (3.14)$$

$$U \cong U^{(0)} + w_i U^{(1)} + w_i^2 U^{(2)} + \cdots \qquad (3.15)$$

$$W \cong w_i \chi^{(1)} + w_i^2 \chi^{(2)} + \cdots \qquad (3.16)$$

where w_i is the local concentration of air at the interface and χ is the normalized concentration function.

By substituting equations (3.6 - 3.16) into equations (3.1 - 3.5), and retaining terms of the lowest order in w_i , one obtains the following system of equations:

$$\frac{d}{dy}(\rho^{(0)} v^{(0)}) = 0 \tag{3.17}$$

$$\rho^{(0)} v^{(0)} \frac{dv^{(0)}}{dy} = -\frac{dp^{(0)}}{dy} + \frac{4}{3}\mu_1 \frac{d^2 v^{(0)}}{dy^2} \tag{3.18}$$

$$\rho^{(0)} v^{(0)} C_{p_1} \frac{dT^{(0)}}{dy} = v^{(0)} \frac{dp^{(0)}}{dy} + K_1 \frac{d^2 T^{(0)}}{dy^2} + \frac{4}{3}\mu_1 \left(\frac{dv^{(0)}}{dy}\right)^2 \tag{3.19}$$

$$p^{(0)} = \rho^{(0)} R_{M_1} T^{(0)} \tag{3.20}$$

$$\rho^{(0)} v^{(0)} \chi^{(1)} = \rho^{(0)} D_{12} \frac{d\chi^{(1)}}{dy} \tag{3.21}$$

The boundary conditions for equations (3.17 - 3.21) are those stated by equations (2.3.5) and (2.3.6). Since we come up with a system identical to that in section (2-3), the linearized solution for the limiting case ($M_\infty \to 0$) is simply written

$$T^{(0)} \cong T_\infty - \left(\frac{T_\infty - T_s}{T_\infty}\right) T_\infty \, e^{-\frac{2}{3}\frac{\bar{G}}{\mu_1} y} \tag{3.22}$$

$$v^{(0)} \cong v_\infty - \left(\frac{T_\infty - T_s}{T_\infty}\right) v_\infty \, e^{-\frac{2}{3}\frac{\bar{G}}{\mu_1} y} \tag{3.23}$$

$$\rho^{(0)} \cong \rho_\infty + \left(\frac{T_\infty - T_s}{T_\infty}\right) \rho_\infty \, e^{-\frac{2}{3}\frac{\bar{G}}{\mu_1} y} \tag{3.24}$$

while the pressure of a mixture is again approximately constant.

By neglecting the small variation of the density, one can rewrite equation (3.21) as

$$\bar{G}\chi^{(1)} \cong -\rho_\infty D_{12} \frac{d\chi^{(1)}}{dy} \tag{3.25}$$

for which the boundary condition is

$$\chi^{(1)} = 1 \qquad at \qquad y = 0 \tag{3.26}$$

Integration of equation (3.25) gives

$$\chi^{(1)} = exp\left(-\frac{\bar{G}}{\rho_\infty D_{12}} y\right) \tag{3.27}$$

and

$$W^{(1)} = W_i \, exp\left(-\frac{\bar{G}}{\rho_\infty D_{12}} y\right) \tag{3.28}$$

Since D_{12} is about the same order of magnitude as ν_1, the thickness of the diffusion layer is found to be comparable to that of a visco-conduction layer.

To calculate W_i, the total amount of air per unit area must be specified. Denoting it by A_g, there is obtained

$$A_g = \int_0^\infty \rho_\infty W_i \, exp\left(-\frac{\bar{G} y}{\rho_\infty D_{12}}\right) dy \tag{3.29}$$

Integration gives

$$A_g = \rho_\infty^2 W_i \frac{D_{12}}{\bar{G}} \tag{3.30}$$

from which one obtains

$$W_i = \frac{A_g \bar{G}}{\rho_\infty^2 D_{12}} \tag{3.31}$$

As can be seen from equation (3.31), for a fixed amount of air A_g and rate of condensation $\bar{G}$, the lower the vapor pressure is, the higher the concentration of air is at the interface. The higher concentration of air at the interface will seriously retard the rate of mass condensation. This fact explains the significance of the presence of noncondensible gases in the system of low pressure metal vapor.

The partial pressure of vapor P_{v_i} at the interface is calculated from

$$P_{v_i} \cong P_\infty \frac{1 - W_i}{1 - (1 - \frac{M_1}{M_2}) W_i} \tag{3.32}$$

By letting

$$\beta_{W_i} = \frac{1 - W_i}{1 - (1 - \frac{M_1}{M_2}) W_i} \tag{3.33}$$

one obtains the important formula for a mixture

$$\beta_{W_i} P_\infty - P_s = \frac{2}{\pi} \bar{G} (2\pi R_{M_1} T_s)^{\frac{1}{2}} \tag{3.34}$$

In contrast to equation (2.4.17) which was obtained for the case of a pure vapor. A comparison of these results for a mixture of mercury and air with experimental data of Sukhatme on a finger type condenser is shown in Figure 10. The finger type condenser will be analyzed and the above comparison will be discussed in the next section.

IV. FILM CONDENSATION OUTSIDE AN ISOTHERMAL VERTICAL TUBE

4.1 Theory

The condensation of low pressure metal vapor on a finger type condenser is illustrated in Fig. 7. There are three regions in which the temperature is gradually brought down to that on the wall. These regions are: (a) the outer region in which the vapor expands isentropically, (b) the interfacial region in which the vapor is slowed down and cooled by the presence of noncondensible gases and by viscosity and heat resistance, and (c) the liquid film region across which the temperature distribution is approximately linear. Since the thickness of the liquid film and interfacial region are very thin compared to the radius of the condensing tube, the flow problem in these two regions can be approximated as condensation on a vertical flat plate. The general analysis and results in Sections II and III can be applied here. On the other hand, the temperature drop in the outer region can be found from the consideration of an inviscid pure vapor. The reason for considering the vapor pure is that almost all the noncondensible gas is in the interfacial region.

The governing equations for the vapor in the outer region are

Continuity:

$$\frac{d}{dr}(\rho v r) = 0 \tag{4.1.1}$$

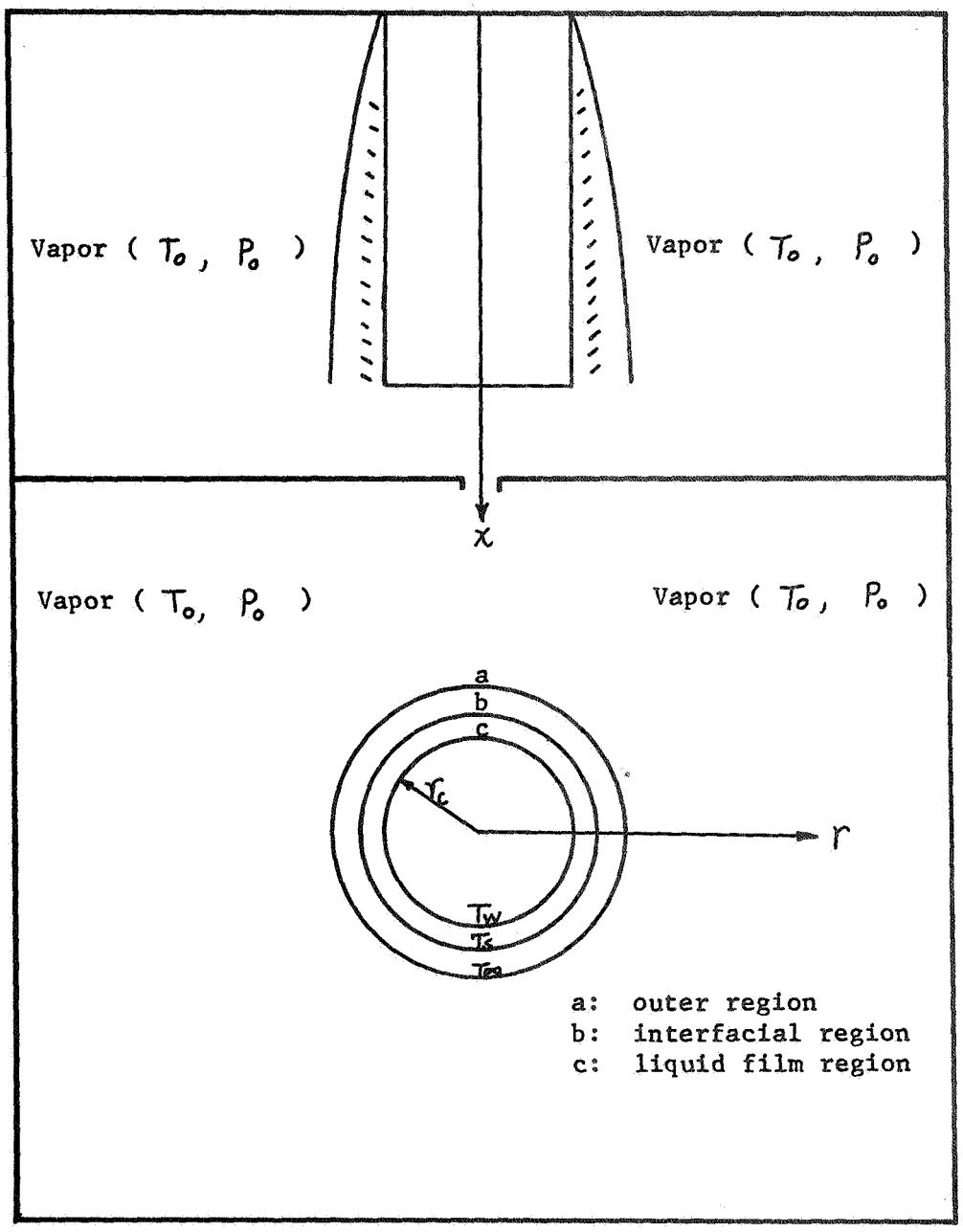

Figure 7. Schematic of finger type condenser

Momentum:

$$\rho v \frac{dv}{dr} = - \frac{dp}{dr} \tag{4.1.2}$$

Energy:

$$\frac{d}{dr}\left(\frac{v^2}{2} + c_p T \right) = 0 \tag{4.1.3}$$

State:

$$p = p_0 \left(\frac{T}{T_0} \right)^{\frac{\gamma}{\gamma-1}} \tag{4.1.4}$$

In these equations, ρ , p and T are respectively the density, pressure and temperature of the vapor, while v is the velocity in the radial direction. Subscript 0 denotes stagnation conditions. The appropriate boundary conditions are:

Stagnation conditions ($r \rightarrow \infty$)

$$T = T_0 \quad , \qquad p = p_0 \tag{4.1.5}$$

Inner condition ($r \cong r_c$)

$$T = T_\infty \tag{4.1.6}$$

where T_∞ is the temperature at the intersection between the

outer and interfacial regions.

The solution for the mass flux per unit area of condensing tube, which is again denoted by $\bar{G}$, is easily obtained by solving the equations (4.1.1-4.1.6)

$$\bar{G} = \rho_o \left[2 C_p (T_o - T_\infty) \right] \left(\frac{T_\infty}{T_o} \right)^{\frac{1}{\gamma - 1}} \tag{4.1.7}$$

For completeness, the results in the liquid film and interfacial regions are rewritten from equations (2.2.16), (2.2.17) and (3.34)

$$\bar{G} = \frac{4}{3} \left(\frac{g \, k_\ell^3 \, \rho_\ell^2}{4 \, \mu_\ell \, \lambda^3 \, L} \right)^{\frac{1}{4}} (T_s - T_w)^{\frac{3}{4}} \tag{4.1.8}$$

and

$$\beta_{w_i} P_\infty - P_s = \frac{2}{\pi} \bar{G} \left(2 \pi R_M T_s \right)^{\frac{1}{2}} \tag{4.1.9}$$

where β_{w_i} is defined by equation (3.33) and

$$P_\infty = P_o \left(\frac{T_\infty}{T_o} \right)^{\frac{\gamma}{\gamma - 1}} \tag{4.1.10}$$

Solving equations (4.1.7-4.1.9) simultaneously, $\bar{G}$, T_∞ and T_s can be determined.

Because of algebraic complications, the theoretical calculation starts with assuming T_∞ . $\bar{G}$ is then calculated from equation (4.1.8). The temperature T_s is obtained from equation (4.1.9).

4.2 Results and Comparisons

Some analytical results of condensation of mercury vapor are shown in Fig. 8, in which the heat flux versus total temperature is plotted for various values of the stagnation pressure.

The length of the condensing tube is chosen to be 6 inches, the length used in Sukhatme's experiments. The properties of Mercury are taken from references [24, 25] and are as follows:

$$C_{p_\ell} = .033 \quad \frac{BTU}{lbm\,^\circ F}$$

$$\rho_\ell = 830 \quad \frac{lbm}{ft^3}$$

$$\nu_\ell = .1 \times 10^{-5} \frac{ft^2}{sec}$$

$$K_\ell = 6.64 \quad \frac{BTU}{hr\ ft\,^\circ F}$$

$$\lambda = 127 \quad \frac{BTU}{lbm}$$

$$M = 201 \quad \frac{lbm}{mole}$$

The saturation pressure as a function of temperature (shown in Figure 9)

The analytical results have been compared with Sukhatme's data for condensation of mercury vapor. In the absence of a noncondensible gas, the theoretical predictions, which are noted by solid lines 1-5 in Fig. 8 are higher than Sukhatme's data by approximately a factor of 2. On the other hand, Nusselt's theory predicts values 8 to 50 times the values obtained from Sukhatme's data.

In Fig. 8, curves 1, 2, and 3 represent those pressures which

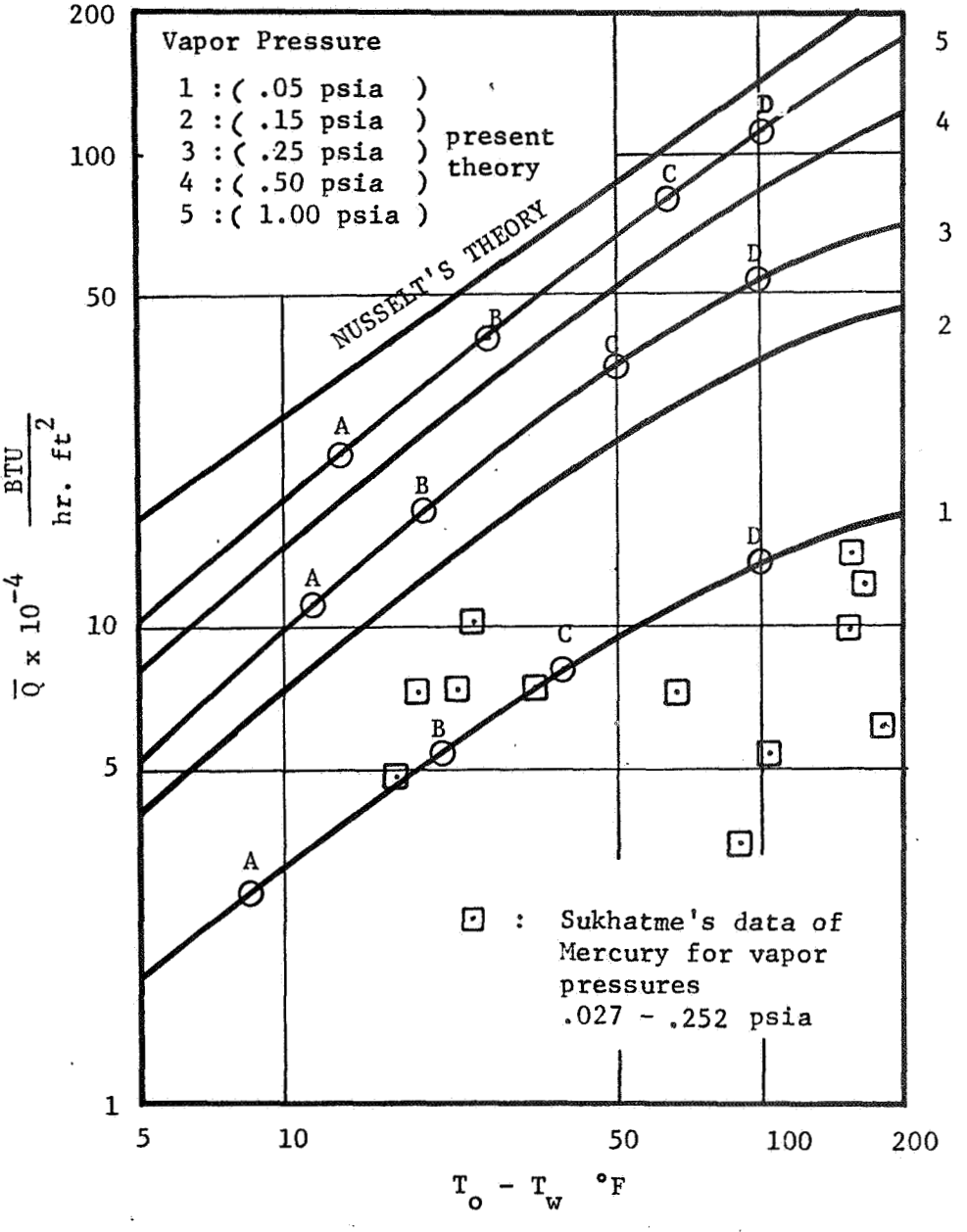

Figure 8. Comparison of experimental data with the present theory neglecting the presence of air.

can be found in Sukhatme's data. Curves 4 and 5 are some higher pressures. It clearly indicates that the present theory approaches Nusselt's theory as the pressure becomes higher.

To show the relative magnitude of the temperature drop in various regions, the temperature drops in these regions are listed in Table I for different values of stagnation pressure. A, B, C and D are the corresponding points shown on lines 1, 3 and 5 in Fig. 8. As can be seen, at lower pressures, the largest temperature drop occurs in the interfacial region. In some situations, the outer region may become equally or even more important than the interfacial region. As pressure becomes higher, the temperature drop in the liquid film becomes the most important.

Better agreement can be obtained by assuming a small amount of air is present in the system. To get agreement with Sukhatme's data, it is necessary to assume there is 4.9×10^{-9} lbm of air present in his chamber, the dimensions of which are 6-in diameter and 11-in length. The corresponding vacuum pressure of air is 4.94×10^{-6} bars. The results obtained by including this amount of air are shown in Fig. 10.

TABLE I. Temperature drop in outer, interfacial and liquid film regions

Stagnation pressure (P_o)	Point	Temperature Drop °F		
		Outer region	Interfacial region	Liquid film region
.05 psia (line 1)	A	2	6	.4
	B	8	12	1.05
	C	18	18	1.8
	D	56	40.3	3.7
.25 psia (line 3)	A	1.5	7.5	2.7
	B	4	11	5
	C	16	21	16
	D	36	37	35
1.00 psia (line 5)	A	.5	5	8
	B	1.5	8.5	17.5
	C	6	15.5	44
	D	12	21.5	72

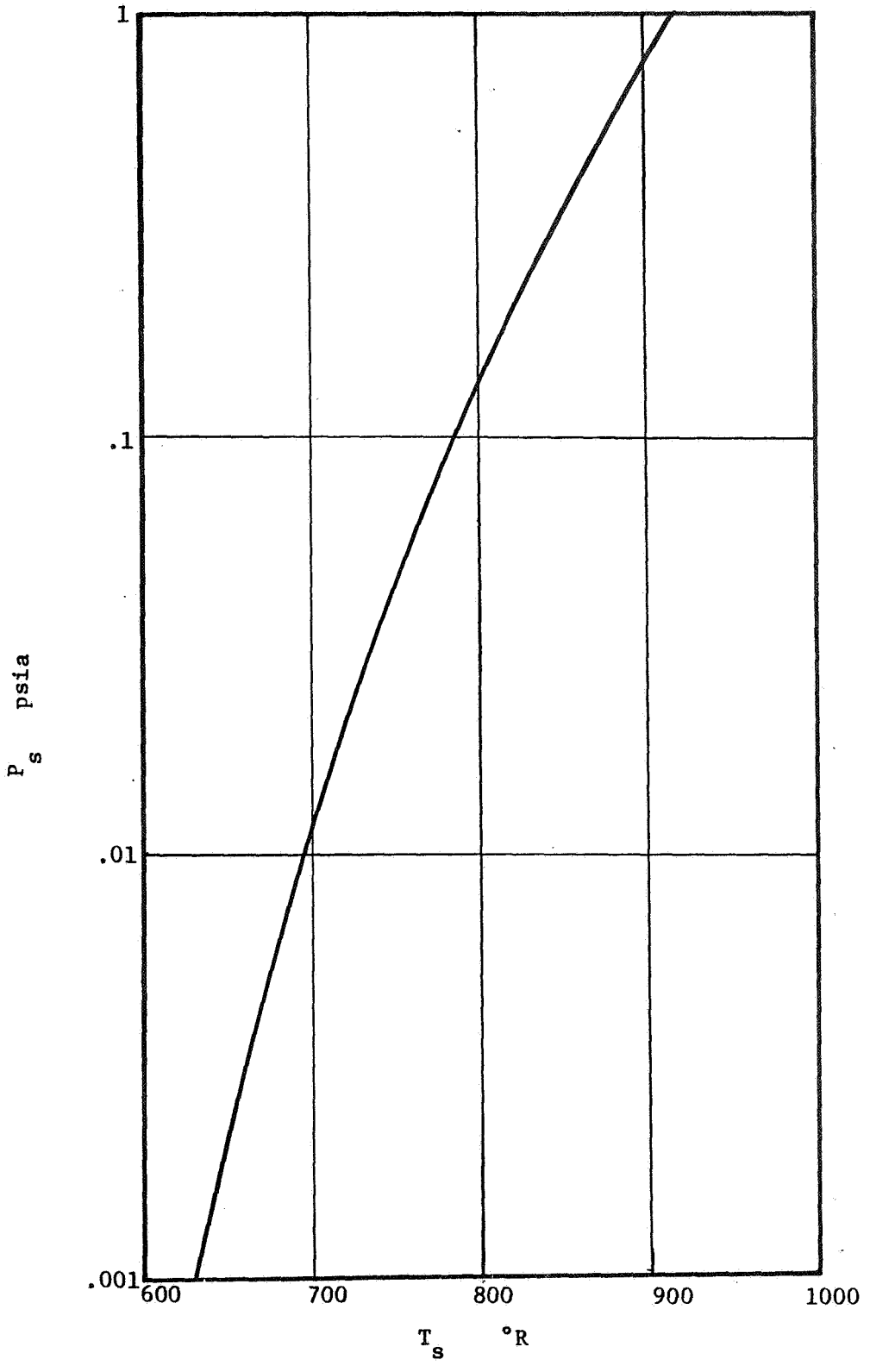

Figure 9. Saturation curve of Mercury (Reference 25)

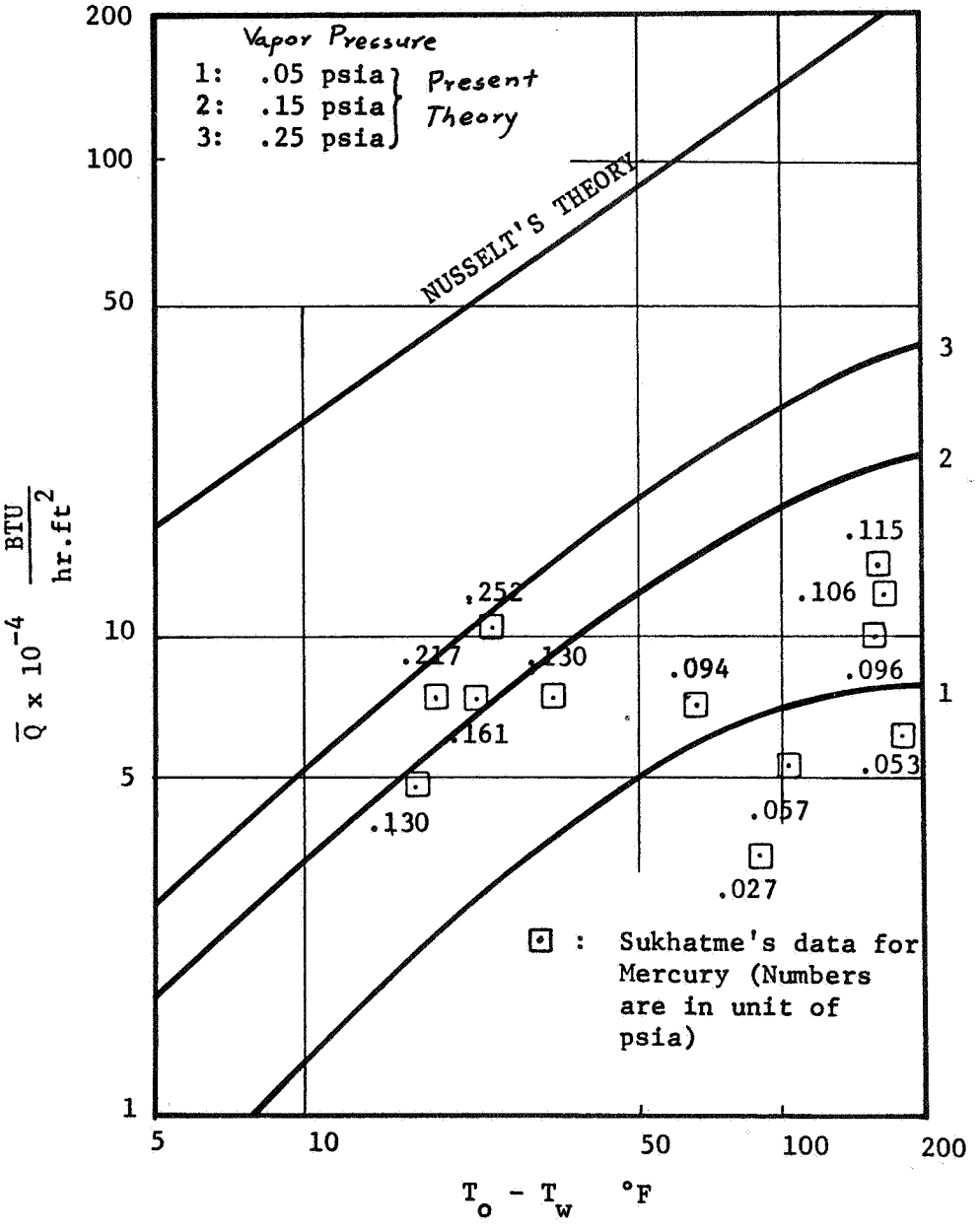

Figure 10. Comparison of experimental data with the present theory including the presence of air

V. DISCUSSION AND CONCLUSIONS

A set of algebraic equations has been found for the prediction of heat transfer rate by condensation. Good agreement has been found between the available data and the theoretical predictions when the presence of a small amount of air was considered.

The theory is limited to small values of $\frac{T_\infty - T_s}{T_\infty}$ and Mach number of the mean vapor flow, but it can be extended to larger values of these parameters by working out higher order solutions. However, a good heat transfer system transfers heat with temperature drops as small as possible. The corresponding Mach number is accordingly very small. Typically, the values of $\frac{T_\infty - T_s}{T_\infty}$ are 0.05 or less and the values of Mach number are 0.2 or less. The error involved in using the linearized analysis may be estimated to be 4% or less, and therefore the linearized solution is valid in most applications.

The approximation of a constant temperature on the surface of the liquid film was validated by Sukhatme's experiment. He measured the thickness distribution of the liquid film and found that it could be described by Nusselt's analysis with an assumed film surface temperature.

Only the solution for small concentration of noncondensible gases was given in this investigation. It was found that the presence of noncondensible gases seriously retards the heat transfer rate of condensation. In experiments, a great deal of care was taken to keep the amount of noncondensible gases small. For this reason,

the solution for small concentration is sufficient. In the calculations, the concentration of air at the liquid-vapor interface is 0.1 or less, which is small.

The effect of free convection has been considered by retaining the body force term in the momentum equation. It was found that free convection will decrease the heat transfer rate slightly, but the correction is very small, about 0.1% or less. For a small temperature drop, the free convection is apparently not important, while for a large temperature drop, the motion due to free convection is still far less important than the induced mean vapor flow.

There are other factors not being considered in the present analysis, for instance the impurity of the vapor, the contamination of the liquid surface, surface tension, and possible nucleation of the vapor near the interface. Intuitively all these factors probably decrease condensation heat transfer. We conclude that the present theory can be used in predicting an upper limit of heat transfer rate due to condensation of low pressure metal vapors.

Some conclusions from the results of this investigation are:

(a) During film condensation of low pressure metal vapor, a significant thermal resistance does exist very near the liquid-vapor interface.

(b) The resistance increases with decreasing vapor pressure. For a high pressure system or non-metal fluids, this resistance becomes negligible and Nusselt's theory is a good approximation.

(c) For a low pressure system, condensation outside a tube decreases seriously due to the expansion of the vapor itself.

(d) The thermal resistance due to the presence of a fixed amount of air increases with decreasing vapor pressure and with increasing molecular weight of a pure vapor. More clearly, the presence of noncondensible gases is less important in steam or in organic vapors than in heavier metal vapors.

(e) The heat transfer coefficient decreases with decreasing vapor pressure. If the weight of a heat transfer system is not an important factor, a low pressure metal vapor is not an efficient working fluid. However, for light-weight systems at very high temperatures, metal vapors become the only possible working fluids.

REFERENCES

1. W. Nusselt, Zeitsch. d. Ver. deusch., vol. 60, 1916, p. 541.

2. L. A. Bromley, Ind. and Eng. Chem., vol. 44, 1952, p. 2966.

3. R. A. Seban, "Remarks on Film Condensation with Turbulent Flow," Trans. ASME, vol. 76, 1954, pp. 299-303.

4. W. M. Rohsenow, "Heat Transfer and Temperature Distribution in Laminar-Film Condensation," Trans. ASME, vol. 78, 1956, pp. 1645-1648.

5. E. M. Sparrow and J. L. Gregg, "A Boundary Layer Treatment of Laminar-Film Condensation," Journal of Heat Transfer, Trans. ASME, Series C, vol. 81, 1959, pp. 13-18.

6. I. Mabuchi, Trans. Japan Soc. Mech. Engrs., vol. 26, 1960, p. 1134.

7. M. M. Chen, "An Analytical Study of Laminar Film Condensation: Part I-Flat Plates," Journal of Heat Transfer, Trans. ASME, Series C, vol. 83, 1961, pp. 48-54.

8. J. C. Y. Koh, E. M. Sparrow, and J. P. Hartnett, Int. J. Heat and Mass Transfer, vol. 2, 1961, p. 69.

9. J. C. Y. Koh, "An Integral Treatment of Two-phase Boundary Layer in Film Condensation," Trans. ASME, Series C, vol. 83, 1961, pp. 359-362.

10. B. Misra and C. F. Bonilla, Chem. Eng. Progr. Sym., Series no. 18, vol. 52, 1956, p. 7.

11. P. D. Cohn, MS thesis, Oregon State College, 1960.

12. S. P. Sukhatme, and W. M. Rohsenow, "Heat Transfer during Film Condensation of a Liquid Metal Vapor," Journal of Heat Transfer, Trans. ASME, Series C, vol. 88, 1966, pp. 19-28.

13. H. Hertz, Ann. Physik v. Chem. (Poggendorf), 17, 1882, pp. 193-200.

14. R. W. Schrage, A Theoretical Study of Interface Mass Transfer, Columbia University Press, New York, N. Y., 1953

15. R. Y. Kucherov, and L. E. Rikenglaz, Zh. eksperim. i. teor. fiziki, 37, no. 1 (7), 1959.

16. D. A. Labuntsov, "An Analysis of Evaporation and Condensation Process," High Temperature, vol. 5, no. 4, 1967, p. 579.

17. A. J. Patton and G. S. Springer, "A Kinetic Theory Description of Liquid-Vapor Phase Change," Sixth Rarefied Gas Dynamics, Conference, 1968.

18. R. E. Barry, "Condensation of Sodium at High Heat Flux," Ph.D. thesis, The University of Michigan, 1965.

19. W. J. Minkowycz and E. M. Sparrow, Int. J. Heat and Mass Transfer, vol. 9, 1966, pp. 1125-1144.

20. A. J. Sartor, R. E. Balzhiser, and R. E. Barry, "Condensing Heat Transfer Considerations Relevant to Rubidium and Other Alkali Metals," Eleventh National Heat Transfer Conference, AIChE. Preprint 5, 1969.

21. Liquid-Metals Handbook, Atomic Energy Commission, June 1952.

22. E. H. Kennard, Kinetic Theory of Gases, McGraw-Hill Book Co., Inc., New York, N. Y., 1938.

23. S. Chapman and T. G. Cowling, The Mathematical Theory of Non-uniform Gases, Cambridge at the University Press, 1953.

24. E. R. G. Eckert and R. M. Drake, Jr., Heat and Mass Transfer, McGraw-Hill Book Co., Inc., New York, N. Y., 1959.

25. J. E. Lay, Thermodynamics, Charles E. Merrill Book, Inc., Columbus, Ohio, 1964.